The International Journal of Cardiovascular Imaging (2019) 35:1221–1229
https://doi.org/10.1007/s10554-019-01545-5

ORIGINAL PAPER

Ventricular geometry–regularized QRSd predicts cardiac resynchronization therapy response: machine learning from crosstalk between electrocardiography and echocardiography

Juan Lei[1,2] · Yi Grace Wang[3] · Luna Bhatta[1] · Jamal Ahmed[1] · Dali Fan[4] · Jingfeng Wang[2] · Kan Liu[1,5]

Received: 3 December 2018 / Accepted: 23 January 2019 / Published online: 18 May 2019

Abstract

Up to one-third of patients selected by current guidelines do not respond to cardiac resynchronization therapy (CRT), the aim of this study was to find out novel analytical approaches to improve pre-implantation CRT response prediction. Among 31 pre-implantation features of clinical, laboratory, electrocardiography (ECG), and echocardiography variables in a consecutive cohort of patients receiving a first-time CRT device (CRT-pacemaker or CRT-defibrillator), we developed a machine learning (ML) model with three classification algorithms (support vector machines (SVM), *K* nearest neighbors, and random subspaces) with the best features combination to predict CRT response. Three categorical variables, left bundle branch block (LBBB), nonischemic cardiomyopathy, and female gender, were independently associated with CRT responses. Among continuous variables, including septal wall thickness, posterior wall thickness, and relative wall thickness (RWT), could regularize ECG QRS duration (QRSd) and significantly enhance the correlation between QRSd and CRT response. The 3 ML algorithms in a total of 38 features combinations constantly recognized that the features combined with QRSd/RWT outperformed the combinations without it. For each of three algorithms, the triplet feature combination of QRSd/RWT, LBBB, and nonischemic cardiomyopathy repeatedly increased the classification rate more than 8%. The best performance for CRT response prediction occurred with SVM model, which proposed actual QRSd/RWT values that favored CRT responses in patients both with and without LBBB. Lower QRSd/RWT values were required for CRT responses in patients with ischemic cardiomyopathy compared to those with non-ischemic cardiomyopathy. ML from ventricular remodeling characteristics–regularized QRSd improves CRT response prediction.

Keywords Cardiac resynchronization therapy · QRS duration · Machine learning · Classification · Ventricular geometric characteristics

✉ Jingfeng Wang
drwjf@hotmail.com

✉ Kan Liu
Kan-Liu@uiowa.edu

[1] Division of Cardiology, Department of Medicine, State University of New York, Upstate Medical University, Syracuse, NY 13202, USA

[2] Department of Cardiology, Sun Yat-Sen Memorial Hospital, Sun Yat-Sen University, Guangzhou 510120, Guangdong, China

[3] Department of Mathematics, California State University Dominguez Hills, Carson, CA, USA

[4] Division of Cardiology, Department of Medicine, University of California, Davis, CA, USA

[5] Division of Cardiology, Department of Medicine, University of Iowa, Iowa City, IA 52242, USA

Introduction

Up to one-third of patients selected by current guidelines do not respond to cardiac resynchronization therapy (CRT), which underscores the need to predict a patient's CRT response with precision before implantation [1–4]. Although electrocardiographic (ECG) QRS duration (QRSd) thresholds are utilized as CRT selection criteria [5–8], QRSd values in patients receiving CRT have been found to be suboptimal markers to either quantify mechanical dyssynchrony or correlate factual CRT responses [9]. Machine learning (ML) is a robust computational approach including a collection of statistical learning and modeling techniques that learn from established data and make predictions on unseen or new data [6]. We apply classification, a ML approach [10–12] for the "best separation" of the intrinsic relations among all

the features in each study group [10], to resolve the intricate correlations between QRSd and clinical/imaging characteristics, so as to improve CRT response prediction.

Methods

Patient selection and study design

Informed consent was obtained from each patient. The study protocol conforms to the ethical guidelines of the 1975 Declaration of Helsinki as reflected in a priori approval by the Institutional Research Board of the Human Subjects Committee of State University of New York (SUNY) Upstate Medical University.

From January 1, 2009 to December 31, 2015 in SUNY Upstate Medical University Hospital, 184 consecutive patients received CRT device implantation in accordance with the American College of Cardiology Foundation/American Heart Association guidelines [2, 5]. After excluding 46 patients receiving CRT device replacement and 21 patients having baseline atrial fibrillation which biventricular capture less than 90%, we eventually enrolled 117 patients. Mean follow-up duration was 33 (6–81) months. CRT response was defined as (1) the improvement in clinical heart failure (HF) symptoms (New York Heart Association (NYHA) functional class increases more than one class), and (2) the reduction of left ventricular (LV) end systolic volume (LVESV) $\geq$ 15% after 6 months of CRT [13].

Clinical and laboratory data

We completed a systematic search of the computerized database EPIC Electronic Medical Record through chart review to obtain data before device implantation and after follow-up. A total of 31 clinical, ECG, and echocardiographic variables were included (Tables 2, 3). The etiologies for HF were classified as ischemic and nonischemic [14]. The NYHA functional class was decided based on the highest functional class reached.

ECG

A 12-lead surface ECG was recorded at 25 mm/s during spontaneous rhythm before implantation of the CRT device. QRSd analysis was performed according to standard protocols [15] and our previous publication [16]. Briefly, the morphology of QRS was classified as either LBBB or non-LBBB (including right bundle branch block and nonspecific intraventricular conduction delay [17]). LBBB was defined as a QRSd > 120 ms; QS or rS in lead V1; broad R waves in leads I, avL, V5, or V6; and absent q waves in leads V5 and V6. QRSd and morphology were measured and assessed electronically, and subsequently confirmed by 2 board-certified cardiologists (JL and BL) independently.

Echocardiography

Two-dimensional (2D) transthoracic echocardiography (TTE) was performed with standard techniques using a GE Vivid E9 machine (GE Healthcare, Vingmed Ultrasound A/S, Norway) with a 3.5-MHz phased-array transducer. Echocardiographic parameters included left atrial (LA) dimension, LV end diastolic dimensions (LVEDD), septal wall thickness (SWT), posterior wall thickness (PWT), LVESV, LV end diastolic volume (LVEDV) and LV ejection fraction (LVEF). The LVEF was calculated by biplane Simpson's method from apical 4- and 2-chamber views. SWT and PWT were assessed by linear measurements in parasternal long-axis view images at the level of the mitral leaflet tips at end-diastole (at the onset of the R wave and LV in the largest dimension) [18]. RWT was calculated as the sum of SWT and PWT divided by LVEDD [19]. LV mass was calculated as $0.8*(1.04*((\mathrm{LVEDD}+\mathrm{PWT}+\mathrm{SWT})^3-(\mathrm{LVEDD})^3))+0.6$ [20]. The rest of the measurements were performed according to American Society of Echocardiography guidelines [18, 21] and our previous publications [22, 23]. Echocardiography data before and after 6-month CRT were recorded. In order to reduce intra- and inter-observer variability, all the measurements were done by the same person (JL), and all the parameters were the mean of 3 measurements.

CRT device implantation

CRT device implantations were performed according to published guidelines [6]. Briefly, a LV lead was inserted transvenously via the subclavian route. A coronary sinus venogram was obtained using a balloon catheter, and the LV pacing lead was inserted through the coronary sinus with the help of an 8-F or 9-F guiding catheter and positioned as far as possible in the venous system, preferably in the lateral or posterolateral vein. The atrial and RV leads were placed regularly at the right atrial appendage and the RV apex. All leads were connected to a dual-chamber biventricular implantable cardiac device. The atrioventricular interval was optimized using Ritter's method with TTE [24].

Statistical analysis

Continuous variables were presented as mean $\pm$ standard deviation (SD) and dichotomous variables as an absolute number with percentage. Comparisons between continuous variables were made using both parametric and nonparametric methods—student's *t*-test and permutation test. Dichotomous variables were compared using chi-squared test. Logistic regression model and univariate and multivariate analyses

were performed to related demographic, clinical, ECG, and echocardiographic parameters to the CRT response. All variables in univariate analysis with a p-value < 0.20 entered multivariate analysis. The variables with p-value < 0.05 were in the final model. Receiver operating characteristic (ROC) analysis were used, and area under the curve (AUC) were calculated. A 2-sided p-value of 0.05 was set as statistically significant. Statistical analyses were performed using SPSS for Windows, version 22.0 (IBM Corporation, Armonk, New York, USA) and R programming 3.2.3 for Windows (UpdateStar Inc., Berlin, Germany).

Machine learning/classification

After selecting appropriate features by standard statistical techniques, the problem was formulated as a supervised learning (classification) problem—a standard problem in ML. Classification approaches learned some predictive models that assigned an observation (a patient with various measurements in our problem) to one of the given classes (responders and non-responders), with the assistance of some labeled observations (whether they were responders or non-responders was known to us). Once the predictive model was obtained, it could be generalized to new observations and predict which class they belong to (Fig. 1). The classification procedures were carried out in MATLAB R2014a with Windows (Mathworks Inc., Natick, Massachusetts, USA).

Results

Demographic and clinical characteristics

Among 117 patients, 72 (61.5%) were male. The average age was 68.5 ± 13.6 years old. Fifty-four patients (46.2%) had nonischemic cardiomyopathy. Seventy-four patients (63.2%) had LBBB. Average QRSd was 161.9 ± 26.6 ms. LVEF (before CRT) was 24.2% ± 7.7%. Eighty-five patients (72.6%) responded to CRT. Compared with CRT non-responders, more CRT responders were female (44.7% vs. 21.9%, $p < 0.05$), had nonischemic cardiomyopathy (54.1% vs 25.0%, $p < 0.01$) and LBBB (71.8% vs 40.6%, $p < 0.01$). There were no significant differences in age, NYHA functional class, concomitant diseases, smoking history, alcohol abuse, lipid level, renal function, and drug treatment between two groups (Table 1).

Feature selection for classification

Among the parameters that could be obtained before CRT implantation (not procedural/device-related parameters, such as lead location, pacing threshold, and % BiV pacing, etc.), we included a total of 31 clinical, laboratory, and echocardiography pre-implantation variables. A nonparametric two-sample test—permutation test—was used to assess the association between continuous variables and the CRT response. Ventricular geometric parameters (SWT and RWT) were found to be significantly related to the CRT response. The correlation between QRSd itself and the CRT response was not significant (Table 2, left column). RWT-, PWT-, and SWT-regularized QRSd were significantly associated with the CRT response (Table 2, right column). Pearson's chi-squared test was used to test the correlations between the categorical variables and the CRT response. LBBB, nonischemic cardiomyopathy, and female gender were found significantly associated with CRT response (Table 3). In the subsequent ML model development, QRSd, RWT, QRSd/RWT, LBBB, nonischemic cardiomyopathy, and female gender served as candidate predictors for the classification problems.

Classification

We investigated the predictive power of different combinations of the candidate features by applying 3 established classification methods, SVM [25], K nearest neighbors (KNN) [26] and random subspaces (RS, an ensemble method) [27] (Fig. 1; implementation details can be found in the "Appendix"). Briefly, by exploring these different classification methods into 1 algorithm, we were able to demonstrate the general predictive power of the features.

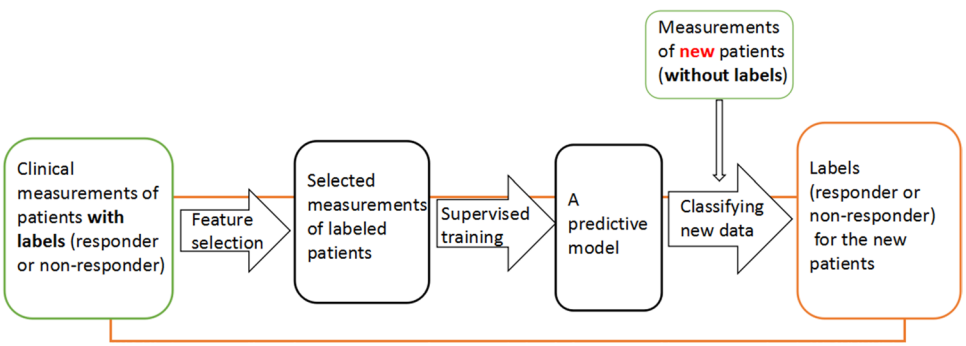

Fig. 1 Classification approaches of building up predictive models

Table 1 Baseline patient characteristics

	CRT responders (n = 85, 72.6%)	CRT non-responders (n = 32, 27.4%)	*p*-value
Female gender (%)	38 (44.7)	7 (21.9)	0.024
Age (years)	67.6 ± 13.4	70.8 ± 14.1	0.259
Nonischemic cardiomyopathy (%)	46 (54.1)	8 (25.0)	0.002
NYHA class	2.70 ± 0.46	2.84 ± 0.47	0.223
Hypertension (%)	68 (81.0)	24 (75.0)	0.479
Diabetes (%)	30 (35.7)	11 (34.4)	0.893
Smoking (%)	27 (32.9)	9 (29.0)	0.692
Alcohol (%)	22 (27.2)	7 (24.1)	0.751
SBP (mmHg)	126.2 ± 20.2	126.1 ± 17.2	0.972
DBP (mmHg)	72.9 ± 11.5	70.8 ± 8.6	0.348
Height (m)	1.69 ± 0.12	1.71 ± 0.12	0.319
Weight (Kg)	83.9 ± 20.9	87.8 ± 40.2	0.505
QRSd (ms)	161.3 ± 25.9	163.4 ± 28.9	0.728
LBBB (%)	61 (71.8)	13 (40.6)	0.000
Cholesterol (mg/dl)	157.4 ± 39.3	137.0 ± 29.7	0.071
Triglyceride (mg/dl)	153.7 ± 115.3	112.0 ± 52.0	0.162
HDL-C (mg/dl)	52.1 ± 19.6	46.3 ± 11.6	0.273
LDL-C mg/dl	90.6 ± 62.8	68.6 ± 26.6	0.186
Creatinine (mg/dl)	1.31 ± 0.87	1.30 ± 0.44	0.935
ACEI/ARB (%)	70 (82.4)	23 (71.9)	0.211
β-blocker (%)	71 (83.5)	26 (81.3)	0.770
Diuretic (%)	66 (77.6)	25 (78.1)	0.956
Spirolactone (%)	26 (30.6)	7 (21.9)	0.351
Digoxin (%)	18 (21.4)	10 (31.3)	0.269

Data are number (%), mean ± SD

ACEI angiotensin-converting enzyme inhibitors, *ARB* angiotensin receptor blocker, *CRT* cardiac resynchronization therapy, *DBP* diastolic blood pressure, *HDL-C* high-density lipoprotein cholesterol, *LBBB* left bundle branch block, *LDL-C* low-density lipoprotein cholesterol, *NYHA* New York Heart Association, *QRSd* QRS duration, *SBP* systolic blood pressure

For instance, if including a specific feature led to improvement in the results of all the three methods, then this feature proved to be powerful in the prediction (and it is not due to the advantage from a specific classification method). Eventually, we proposed the separating strategy obtained by the method that gave the best result.

On the other hand, we randomly split our data into ten subsets. In each experiment, we held out one subset for validation and learned the predictive model (by the three classification methods) from the rest of the data. Then the accuracy of the predictive model was evaluated using the held-out subset of the data (Fig. 1). The final result we report in Table 4 is the average of ten such experiments (holding out different subsets for validation). This procedure is known as cross-validation in the field of ML (more details can be found in the "Appendix").

Table 2 Test of association between continuous variables and the CRT response (left) and between regularized QRSd and the CRT response (right) (sorted by *p* value from small to large)

Variables	*p* value	Regularized QRSd	*p* value
RWT	0.021	QRSd/RWT	0.003
SWT	0.029	QRSd/PWT	0.005
Cholesterol	0.072	QRSd/SWT	0.005
LVEF	0.087	QRSd/LDL-C	0.070
PWT	0.093	QRSd/LVEF	0.109
LVEDD	0.124	QRSd/cholesterol	0.140
LVEDV	0.142	QRSd/LVEDV	0.179
LA	0.153	QRSd/DBP	0.285
Triglyceride	0.167	QRSd/LVEDD	0.324
LDL-C	0.187	QRSd/LVESV	0.341
Age	0.267	QRSd/HDL-C	0.374
HDL-C	0.286	QRSd/triglyceride	0.410
Height	0.325	QRSd/LA	0.422
DBP	0.346	QRSd/age	0.727
LVESV	0.475	QRSd/height	0.817
Weight	0.517	QRSd/weight	0.904
QRSd	0.732	QRSd/SBP	0.948
Creatinine	0.946	QRSd/creatinine	0.979
SBP	0.975		

CRT cardiac resynchronization therapy; DBP: diastolic blood pressure, *HDL-C* high-density lipoprotein cholesterol, *LA* left atrial, *LDL-C* low-density lipoprotein cholesterol, *LVEDD* left ventricular end diastolic diameter, *LVEDV* left ventricular end diastolic volume, *LVEF* left ventricular ejection fraction, *LVESV* left ventricular end systolic volume, *PWT* posterior wall thickness, *QRSd* QRS duration, *RWT* relative wall thickness, *SBP* systolic blood pressure, *SWT* septal wall thickness

Table 3 Test of association between categorical variables and the CRT response (sort by *p* value from small to large)

Categorical variables	*p* value
LBBB	0.001
Nonischemic cardiomyopathy	0.003
Female gender	0.035
ACEI/ARB	0.303
Digoxin	0.322
Spirolactone	0.368
Hypertension	0.616
β-blocker	0.787
Alcohol	0.810
Smoking	0.820
Diabetes	1.000
Diuretic	1.000

ACEI angiotensin-converting enzyme inhibitors, *ARB* angiotensin receptor blocker, *CRT* cardiac resynchronization therapy, *LBBB* left bundle branch block

Table 4 Classification rate* (%) (test rate) while using different combinations of features

Features/methods	Size[a] (n)	Naïve rate[b] (%)	SVM-RBF (%)	KNN (%)	Random subspace (%)
One feature					
RWT	91	74.73	75.82	75.82	73.63
QRSd	105	72.38	72.38	72.38	72.38
QRSd/RWT	84	73.81	78.57	76.19	77.38
Female	117	72.65	72.65	72.65	72.65
LBBB	103	72.82	72.82	73.79	69.90
Nonischemic cardiomyopathy	113	71.68	71.68	71.68	71.68
Two features					
RWT, QRSd	84	73.81	75.00	73.81	73.81
RWT, Female	91	74.73	76.92	78.02	74.73
RWT, LBBB	82	75.61	81.71	78.05	76.83
RWT, nonischemic cardiomyopathy	88	73.86	80.68	80.68	79.55
QRSd, female	105	72.38	72.38	72.38	72.38
QRSd, LBBB	98	73.47	75.51	73.47	73.47
QRSd, nonischemic cardiomyopathy	103	71.84	73.79	72.82	71.84
QRSd/RWT, female	84	73.81	78.57	77.38	77.38
QRSd/RWT, LBBB	80	75.00	82.50	80.00	81.25
QRSd/RWT, nonischemic cardiomyopathy	83	73.49	79.52	77.11	80.72
Female, LBBB	103	72.82	76.70	76.70	76.70
Female, nonischemic cardiomyopathy	113	71.68	72.57	72.57	71.68
LBBB, nonischemic cardiomyopathy	99	71.72	72.73	72.73	73.74
Three features					
RWT, QRSd, female	84	73.81	73.81	73.81	73.81
RWT, QRSd, LBBB	80	75.00	78.75	76.25	76.25
RWT, QRSd, nonischemic cardiomyopathy	83	73.49	79.52	78.31	79.52
RWT, female, LBBB	82	75.61	78.05	75.61	75.61
RWT, female, nonischemic cardiomyopathy	88	73.86	81.82	80.68	77.27
RWT, LBBB, nonischemic cardiomyopathy	79	74.68	82.28	79.75	75.95
QRSd, female, LBBB	98	73.47	75.51	74.49	74.49
Qrsd, female, nonischemic cardiomyopathy	103	71.84	76.70	75.73	71.84
QRSd, LBBB, nonischemic cardiomyopathy	96	72.92	76.04	77.08	72.92
QRSd/RWT, female, LBBB	80	75.00	76.25	76.25	77.50
QRSd/RWT, female, nonischemic cardiomyopathy	83	73.49	79.52	78.31	79.52
QRSd/RWT, LBBB, nonischemic cardiomyopathy[c]	79	74.68	84.81	82.28	81.01
Female, LBBB, nonischemic cardiomyopathy	99	71.72	75.76	76.77	75.76
Four features					
RWT, QRSd, female, LBBB	80	75.00	76.25	75.00	75.00
RWT, Qrsd, female, nonischemic cardiomyopathy	83	73.49	79.52	78.31	78.31
RWT, QRSd, LBBB, nonischemic cardiomyopathy	79	74.68	82.28	79.75	77.22
RWT, female, LBBB, nonischemic cardiomyopathy	79	74.68	81.01	77.22	75.95
QRSd, female, LBBB, nonischemic cardiomyopathy	96	72.92	79.17	76.04	73.96
QRSd/RWT, female, LBBB, nonischemic cardiomyopathy	79	74.68	83.54	77.22	81.01

*These rates are averaged testing rates, that is, we train the model using training set and test their accuracy on an independent test set. These rates reflect how well the trained model could be generalized to new patients

KNN K-nearest neighbors *LBBB* left bundle branch block, *PWT* posterior wall thickness *QRSd* QRS duration, *RWT* relative wall thickness; SVM-RBF: support vector machines with radial basis function kernel, *SWT* septal wall thickness

[a]Size is the number of patients in the experiments. Due to the removal of missing data, sizes of different combinations are varied

[b]Naïve rate is the percentage of responders to all patients. Following the above trained model, this responding rate can be raised to the reported classification rate

[c]This combination seems to be the best for two reasons. First, the classification rate improves by about 10% at best (for SVM-LBF). Second, the classification rates of improve by about 8% for all the three methods

The best-performing model was developed with SVM. We plotted the improvement (the increase of the classification rate) over the naïve rate in the following way: For each feature, we took all the combinations containing this feature, sorted their SVM improvements, and then plotted these sorted numbers (Fig. 2a). The feature QRSd/RWT exhibited the strongest predictive power for CRT response. All of the combinations with QRSd/RWT outperformed the combinations without it. The next three powerful features were RWT, nonischemic cardiomyopathy, and LBBB.

The combination of QRSd/RWT, LBBB, and nonischemic cardiomyopathy gave the best performance, whose classification rate increased (from the naïve rate/rate of responders in all patients) about 8% with each of the three different classification methods. Applying SVM to these three features indeed improved the classification rate by 10% (from 74.68 to 84.81%) (Table 4). The AUC of combine with QRSd/RWT was significantly greater than that of combine with QRSd (Fig. 2b).

In the SVM method, we plotted the decision boundaries for ischemic and nonischemic cardiomyopathy, respectively (Table 5; Fig. 3). This procedure provided different cut-off values of QRSd/RWT for patients with different states of LBBB and nonischemic cardiomyopathy. The sensitivity and specificity obtained by this procedure are 96.6% and 50.0%, respectively.

Table 5 A summary of the classification procedure obtained by applying SVM to QRSd/RWT, LBBB and nonischemic cardiomyopathy

Nonischemic cardiomyopathy	LBBB	QRSd/RWT (x)	CRT response
0	0	$x<442$	1
		$x>442$	0
	1	$x<719$	1
		$x>719$	0
1	0	$x<636$	1
		$x>636$	0
	1	$x<923$	1
		$x>923$	0

0 means no; and 1 means yes

CRT cardiac resynchronization therapy *LBBB* left bundle branch block *QRSd* QRS duration, *RWT* relative wall thickness, *SVM* support vector vachines

Discussion

The present study demonstrates that different ventricular remodeling patterns correlate with distinctive CRT responses in patients with late-stage HF, and ML from ventricular geometric characteristics–regularized QRSd contributes to CRT response prediction.

Compared to real-time functional assessment, ventricular geometric characteristics mirror cumulative myocardial/structural remodeling effects and better stage chronic HF [28]. Although non-uniform ventricular radius of curvature and regional shape deformation are commonly seen in a remodeling heart, septal and lateral walls are usually subjected to greater wall stress than anterior and inferior walls in late-stage systolic HF [29], therefore the change of the regional wall thickness is particularly prominent for septal and lateral walls [28]. RWT has been increasingly used to reflect dyssynchronous temporal phases of ventricular wall hypertrophy and chamber dilation and discriminate

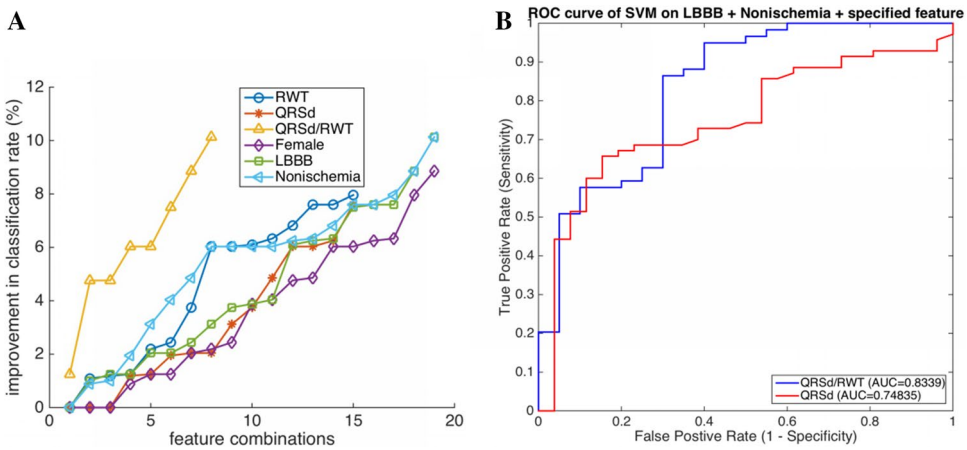

Fig. 2 **a** QRSd/RWT enhanced the power of QRSd to predict CRT response. The feature QRSd/RWT had the best predictive power, followed by nonishchemia, RWT, and LBBB. **b** The ROC curve of SVM on LBBB and nonischemic cardiomyopathy combine with a specified feature. The AUC combined with QRSd/RWT is larger than the AUC combined with QRSd (0.834 vs. 0.748). *AUC* area under the ROC curve, *CRT* cardiac resynchronization therapy, *LBBB* left bundle branch block, *QRSd* QRS duration, *ROC* receiver operating characteristic, *RWT* relative wall thickness, *SVM* support vector machines

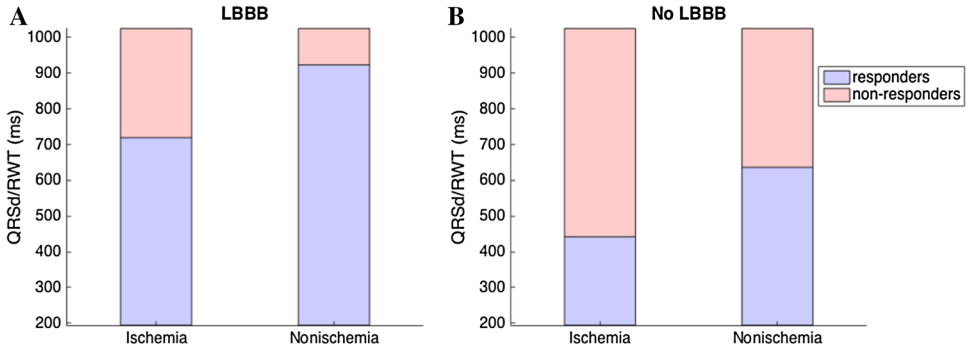

Fig. 3 The cut-off values of QRSd/RWT for patients with different etiologies in predicting CRT response. The different values are shown for ischemic and nonischemic cardiomyopathy patients with (**a**) or without (**b**) LBBB. *LBBB* left bundle branch block, *QRSd* QRS duration, *RWT* relative wall thickness

ventricular structural remodeling stages [28, 30]. The prognostic roles of different ventricular structural remodeling patterns in advanced HF have drawn particular attention when adverse cardiovascular events and outcomes were found to be more frequent in patients with eccentric hypertrophy and reduced RWT [19, 28, 31]. The present study correlated different ventricular structural remodeling patterns with distinctive CRT responses, and its results contradict a traditionally "leitmotiv" concept: "the sickest hearts benefit the most" from CRT [32]. When adverse myocardial remodeling impairs myocardial mechanics to some extent, there is no further therapeutic benefit because the heart becomes too "sick" to respond to CRT.

QRSd thresholds have been utilized for CRT eligibility for a long time [5, 6], and QRSd values are sometimes assumed to reflect the severity of electronic conduction dyssynchrony in CRT-eligible patients. Nonetheless, QRSd values are neither proportional to mechanical dyssynchrony [9] nor consistent with factual CRT responses [28]. In patients with either QRSd between 120 and 150 ms, or QRSd > 150 ms, about 30% constantly failed to demonstrate mechanical dyssynchrony [8]. Extreme QRSd elongation (> 200 ms) was found to be inversely correlated to CRT response [32].

In patients with late-stage HF, QRSd values are significantly affected by ventricular structural alterations. While both ventricular wall hypertrophy and chamber dilation elongate QRSd, the effect from chamber dilation appears to be more prominent [30]. In patients with advanced myocardial remodeling, the "non-electronic dyssynchrony" components could increasingly contribute to the added values of QRSd. In our study, QRSd itself did not significantly correlate with the CRT response. However, regularized QRSd, by ventricular geometric characteristics, became significantly associated with the CRT response. Ventricular geometric characteristics regularization likely helped boost the intrinsic linkages of QRSd and CRT response.

Other than overt ventricular structural changes, covert myocardial substrate characteristics might also affect QRSd. Myocardial fibrosis/scar interferes with the propagation of electronic activation, resulting in heterogeneous activation sequences and QRSd changes [33]. In our study, patients with high QRSd values often had reduced RWT, but the correlation was not linear (data not shown). For CRT response, QRSd/RWT exhibits a stronger predictive power than QRSd itself, implying an inherent linkage between myocardial remodeling and electronic conduction abnormality. Exploring the cross-talk between the ECG and anatomic imaging information helps sort out their promiscuous correlations.

ML is a robust computational approach including a collection of statistical learning and modeling techniques that learn from established data and make predictions on unseen or new data [6]. Compared to classical statistical methodologies, classification/ML focuses on finding the "best separation", instead of the "best summary", of the intrinsic relations among all the features in each group [10]. During ML, the accuracy was evaluated on a different subset of the data, independent from the subset used to determine the model. This accuracy gave a good estimation on how well the model could be generalized to future new observations. In our study, the best performance for CRT response prediction occurred while integrating the numerical measure of QRSd/RWT with two categorical parameters, LBBB and nonischemic cardiomyopathy. Based on presumptively adjusted patient selection criterion, 84.81% (instead of 74.68%) of the CRT-eligible patients became CRT responders (Table 4).

CRT non-responders had relatively high QRSd/RWT values throughout all patient groups (LBBB and non-LBBB, ischemic and nonischemic cardiomyopathy). Patients with LBBB had inclination to respond to CRT. But those LBBB patients with extremely high QRSd/RWT values (with a "dilation without hypertrophy" ventricular geometry) still did not respond, reflecting their irreversible HF status and limited pump function reserve. The cut-off QRSd/RWT values to predict CRT responses were significantly lower in patients with ischemic cardiomyopathy, suggesting that ischemic burden/myocardial scar/fibrosis might essentially impede CRT responses during early ventricular remodeling stages.

Our study has several limitations. It is just an initial effort to apply ML/classification for data analysis and model construction to improve current CRT response prediction. In order to standardize echocardiographic measurements and

maintain consistency of data collection/analysis, we limited this study strictly to a tertiary cardiovascular center. Nevertheless, the single-centered and retrospective nature of this study warrants further validation. Both ventricular geometric characteristics and the ML/classification methodology itself need be validated in future multi-center prospective trials for their roles in improving CRT response prediction and reducing non-responders.

Conclusion

ML from ventricular remodeling characteristics–regularized QRSd improves CRT response prediction.

Compliance with ethical standards

Conflict of interest The authors report no conflicts of interest in this study.

Appendix

Supplemental methods

For SVM, radial kernel was used. Mahalanobis distance was used in KNN. For all of the three methods, cross-validation was applied to choose appropriate values of the parameters.

Cross-validation, a well-known model/parameter selection technique, was performed to select appropriate parameters and estimate the test classification error. More specifically, we randomly split the whole data into ten subsets. For each experiment, nine of subsets were used as training data and the remaining one was used as test data. In other words, the features and the corresponding labels of training data were used to learn the model and then this model was applied to the features of test data to predict the response. The predicted labels were then compared with the ground truth to compute the test classification rate. The subset for testing is then permuted and ten experiments are carried out. The report classification rate is the average over ten experiments.

The advantage of cross-validation is twofold. First, the best model and parameter can be determined using the training data. Second, there was no overlap between the training and test data, and the ground-truth labels of the test data were not used for predicting the labels. Therefore, the test classification rate computed through the above procedure was a good measure about how well the model performs on further unseen data. Furthermore, the data are split at random and the subset for testing is permuted. It is well known that the variation in the averaged test classification rate is small.

References

1. Goldenberg I, Kutyifa V, Klein HU et al (2014) Survival with cardiac-resynchronization therapy in mild heart failure. N Engl J Med 370:1694–1701. https://doi.org/10.1056/NEJMoa1401426
2. Hunt SA, (2005) ACC/AHA 2005 guideline update for the diagnosis and management of chronic heart failure in the adult: a report of the American College of Cardiology/American Heart Association task force on practice guidelines (writing committee to update the 2001 guidelines for the evaluation and management of heart failure). J Am Coll Cardiol 46:e1–e82. https://doi.org/10.1016/j.jacc.2005.08.022
3. Cleland JG, Freemantle N, Erdmann E et al (2012) Long-term mortality with cardiac resynchronization therapy in the cardiac resynchronization-heart failure (CARE-HF) trial. Eur J Heart Fail 14:628–634. https://doi.org/10.1093/eurjhf/hfs055
4. Manlucu J, Tang AS (2014) Whom should I refer in 2014 for cardiac resynchronization? Can J Cardiol 30:675–678. https://doi.org/10.1016/j.cjca.2014.03.019
5. Yancy CW, Jessup M, Bozkurt B et al (2013) 2013 ACCF/AHA guideline for the management of heart failure: a report of the American College of Cardiology Foundation/American Heart Association task force on practice guidelines. Circulation 128:1810–1852. https://doi.org/10.1161/CIR.0b013e31829e8807
6. Ponikowski P, Voors AA, Anker SD, et al (2016) 2016 ESC guidelines for the diagnosis and treatment of acute and chronic heart failure: the task force for the diagnosis and treatment of acute and chronic heart failure of the European Society of Cardiology (ESC) developed with the special contribution of the Heart Failure Association (HFA) of the ESC. Eur Heart J 37:2129–2200. https://doi.org/10.1093/eurheartj/ehw128
7. Varma N, Manne M, Nguyen D et al (2014) Probability and magnitude of response to cardiac resynchronization therapy according to QRS duration and gender in nonischemic cardiomyopathy and LBBB. Heart Rhythm 11:1139–1147. https://doi.org/10.1016/j.hrthm.2014.04.001
8. Yancy CW, McMurray JJ (2013) ECG—still the best for selecting patients for CRT. N Engl J Med 369:1463–1464. https://doi.org/10.1056/NEJMe1310406
9. Bleeker GB, Schalij MJ, Molhoek SG et al (2004) Relationship between QRS duration and left ventricular dyssynchrony in patients with end-stage heart failure. J Cardiovasc Electrophysiol 15:544–549. https://doi.org/10.1046/j.1540-8167.2004.03604.x
10. Bishop CM (2006) Pattern recognition and machine learning (information science and statistics). Springer, New York
11. Obermeyer Z, Emanuel EJ (2016) Predicting the future—big data, machine learning, and clinical medicine. N Engl J Med 375:1216–1219. https://doi.org/10.1056/NEJMp1606181
12. Sengupta PP, Huang YM, Bansal M et al (2016) Cognitive machine-learning algorithm for cardiac imaging: a pilot study for differentiating constrictive pericarditis from restrictive cardiomyopathy. Circ Cardiovasc Imaging 9:e004330. https://doi.org/10.1161/CIRCIMAGING.115.004330
13. Ellenbogen KA, Huizar JF (2012) Foreseeing super-response to cardiac resynchronization therapy: a perspective for clinicians. J Am Coll Cardiol 59:2374–2377. https://doi.org/10.1016/j.jacc.2011.11.074
14. Felker GM, Shaw LK, O'Connor CM (2002) A standardized definition of ischemic cardiomyopathy for use in clinical research.

J Am Coll Cardiol 39:210–218. https://doi.org/10.1016/S0735-1097(01)01738-7
15. Gold MR, Thebault C, Linde C et al (2012) The effect of QRS duration and morphology on cardiac resynchronization therapy outcomes in mild heart failure: results from the resynchronization Reverses remodeling in systolic left ventricular dysfunction (REVERSE) study. Circulation 126:822–829. https://doi.org/10.1161/CIRCULATIONAHA.112.097709
16. Wang YG, Wu HT, Daubechies I et al (2015) Automated J wave detection from digital 12-lead electrocardiogram. J Electrocardiol 48:21–28. https://doi.org/10.1016/j.jelectrocard.2014.10.006
17. Surawicz B, Childers R, Deal BJ et al (2009) AHA/ACCF/HRS recommendations for the standardization and interpretation of the electrocardiogram, part III: intraventricular conduction disturbances a scientific statement from the American Heart Association Electrocardiography and Arrhythmias Committee, Council on Clinical Cardiology; the American College of Cardiology Foundation; and the Heart Rhythm Society endorsed by the International Society for Computerized Electrocardiology. J Am Coll Cardiol 53:976–981. https://doi.org/10.1016/j.jacc.2008.12.013
18. Lang RM, Bierig M, Devereux RB et al (2005) Recommendations for chamber quantification: a report from the American Society of Echocardiography's Guidelines and Standards Committee and the Chamber Quantification Writing Group, developed in conjunction with the European Association of Echocardiography, a branch of the European Society of Cardiology. J Am Soc Echocardiogr 18:1440–1463. https://doi.org/10.1016/j.echo.2005.10.005
19. Biton Y, Goldenberg I, Kutyifa V et al (2016) Relative wall thickness and the risk for ventricular tachyarrhythmias in patients with left ventricular dysfunction. J Am Coll Cardiol 67:303–312. https://doi.org/10.1016/j.jacc.2015.10.076
20. Devereux RB, Alonso DR, Lutas EM et al (1986) Echocardiographic assessment of left ventricular hypertrophy: comparison to necropsy findings. Am J Cardiol 57:450–458. https://doi.org/10.1016/0002-9149(86)90771-X
21. Nagueh SF, Appleton CP, Gillebert TC et al (2009) Recommendations for the evaluation of left ventricular diastolic function by echocardiography. J Am Soc Echocardiogr 22:107–133. https://doi.org/10.1016/j.echo.2008.11.023
22. Lei J, Dhamoon AS, Wang JF et al (2016) Walking the tightrope: using quantitative Doppler echocardiography to optimize ventricular filling pressures in patients hospitalized for acute heart failure. Eur Heart J Acute Cardiovasc Care 5:130–140. https://doi.org/10.1177/2048872615573517
23. Lei J, Wang JF, Voelker R et al (2014) Developing integrated echocardiographic protocol to optimize cardiac resynchronization therapy with quadripolar lead. J Am Coll Cardiol 64 (16 Supplement): C159. https://doi.org/10.1016/j.jacc.2014.06.732
24. Jansen AH, Bracke FA, van Dantzig JM et al (2006) Correlation of echo-Doppler optimization of atrioventricular delay in cardiac resynchronization therapy with invasive hemodynamics in patients with heart failure secondary to ischemic or idiopathic dilated cardiomyopathy. Am J Cardiol 97:552–557. https://doi.org/10.1016/j.amjcard.2005.08.076
25. Cortes C, Vapnik V (1995) Support-vector networks. Mach Learn 20:273–297. https://doi.org/10.1007/BF00994018
26. Cover T, Hart P (1967) Nearest neighbor pattern classification. IEEE Trans Inf Theory 13:21–27. https://doi.org/10.1109/tit.1967.1053964
27. Ho TK (1998) The random subspace method for constructing decision forests. IEEE Trans Pattern Anal Mach Intell 20:832–844. https://doi.org/10.1109/34.709601
28. Gaasch WH, Zile MR (2011) Left ventricular structural remodeling in health and disease: with special emphasis on volume, mass, and geometry. J Am Coll Cardiol 58:1733–1740. https://doi.org/10.1016/j.jacc.2011.07.022
29. Zhang Q, Fung JW, Auricchio A et al (2006) Differential change in left ventricular mass and regional wall thickness after cardiac resynchronization therapy for heart failure. Eur Heart J 27:1423–1430. https://doi.org/10.1093/eurheartj/ehi885
30. Chan DD, Wu KC, Loring Z et al (2014) Comparison of the relation between left ventricular anatomy and QRS duration in patients with cardiomyopathy with versus without left bundle branch block. Am J Cardiol 113:1717–1722. https://doi.org/10.1016/j.amjcard.2014.02.026
31. Draper TS Jr, Silver JS, Gaasch WH (2015) Adverse structural remodeling of the left ventricle and ventricular arrhythmias in patients with depressed ejection fraction. J Card Fail 21:97–102. https://doi.org/10.1016/j.cardfail.2014.10.018
32. Gasparini M, Galimberti P (2013) Device therapy in heart failure: has CRT changed "the sickest benefit the most" to "the healthiest benefit the most?". J Am Coll Cardiol 61:945–947. https://doi.org/10.1016/j.jacc.2012.11.048
33. Adelstein EC, Saba S (2007) Scar burden by myocardial perfusion imaging predicts echocardiographic response to cardiac resynchronization therapy in ischemic cardiomyopathy. Am Heart J 153:105–112. https://doi.org/10.1016/j.ahj.2006.10.015